Hindawi Publishing Corporation
Mathematical Problems in Engineering
Volume 2016, Article ID 4017076, 12 pages
http://dx.doi.org/10.1155/2016/4017076

Research Article

Analytical and Numerical Study on Magnetoconvection Stagnation-Point Flow in a Porous Medium with Chemical Reaction, Radiation, and Slip Effects

H. Niranjan,[1,2] S. Sivasankaran,[2] and M. Bhuvaneswari[3]

[1]*School of Engineering, Asia Pacific University of Technology and Innovation, 57000 Kuala Lumpur, Malaysia*
[2]*Institute of Mathematical Sciences, University of Malaya, 50603 Kuala Lumpur, Malaysia*
[3]*Department of Mechanical Engineering, University of Malaya, 50603 Kuala Lumpur, Malaysia*

Correspondence should be addressed to S. Sivasankaran; sd.siva@yahoo.com

Received 24 December 2015; Revised 19 March 2016; Accepted 27 March 2016

Academic Editor: Vassilios C. Loukopoulos

We investigate the effects of slip and radiation on magnetoconvection flow of a chemically reacting fluid near a stagnation-point towards a vertical plate embedded in a porous medium analytically and numerically. The governing partial differential equations are diminished into the coupled ordinary differential equations by similarity transformations. Then they are solved analytically by homotopy analysis method and solved numerically by shooting method with RK fourth-order method. In this study, the analytical and numerical results are compared for many combinations of parameters. The rates of heat and mass transfer are calculated. The velocity profile near the plate overshoots on increasing the slip parameter. The concentration and temperature are decreasing on increasing the slip parameter.

1. Introduction

The study of convective heat transfer through porous medium for an incompressible fluid on the heated surface has received major attention because of its diverse uses in the insulation of nuclear reactors, petroleum industry, geothermal problems, storage of nuclear waste, and several other areas. The study of slip condition on convective boundary layer flow beside a vertical plate embedded in a porous medium has accepted considerable practical and theoretical awareness. The research has been maintained out in this area to analyze the heat and mass transfer characteristics within the boundary layer flow. Hiemenz [1] is the pioneer to investigate the forced convection two-dimensional flow at stagnation-point by similarity transformation. Many researchers extended Crane's [2] problem of steady flow of an incompressible fluid over a linearly stretched plate to analyze several conditions. Mohammadi [3] numerically analyzed on boundary layer natural convection flow along a vertical plate. Cheng et al. [4] developed an analytic solution by homotopy analysis method for an unsteady mixed convection flow near the stagnation-point towards a vertical surface in a porous medium. Layek et al. [5] studied the boundary layer flow near stagnation-point in a porous medium over a stretching sheet with heat generation and blowing/suction. Lee et al. [6] studied convective heat transfer over a persuaded plate in a porous medium using Lie group analysis. They perceived that the thickness of the thermal and momentum boundary layer increases on increasing the radiation parameter. The natural convection flow over a plate in a porous medium was examined by Ferdows et al. [7], Rosali et al. [8], and Hou [9]. Bhuvaneswari et al. [10] studied the internal heat generation effect on natural convective flow over an inclined surface in a porous medium. They observed that the profiles of velocity and temperature increase on increasing the heat generation parameter.

The research on magnetohydrodynamic (MHD) flow and heat transfer has several applications in engineering fields such as power generator, design of MHD accelerators, cooling of nuclear reactors, and heat exchangers. The effect

of radiation on heat and mass transfer is essential in some applications, such as hydrometallurgical industries, solar power technology, and astrophysical flows. Takhar et al. [11] and Aydin and Kaya [12] explored the mixed magnetoconvection of a viscous fluid in the surrounding area of a stagnation-point next to a heated vertical surface. Hayat et al. [13] considered the mixed convection stagnation-point flow towards a sheet in a porous medium with magnetic field and radiation effects using homotopy analysis method. Makinde [14] studied the effects of internal heat generation and radiation on MHD mixed convection stagnation-point flow in a perpendicular plate embedded in a porous medium.

The study of chemical reaction on heat and mass transfer is very significant in chemical technology and food processing. Bhuvaneswari et al. [15] studied the effect of chemical reaction on a semi-infinite inclined surface using Lie group analysis. Bhattacharyya [16] and Afify and Elgazery [17] investigated the two-dimensional flow of a viscous fluid with chemical reaction over a stretching/shrinking sheet near a stagnation-point. Recently, boundary layer flow with slip condition has attracted many researchers. Abel and Mahesha [18] analyzed the characteristics of MHD flow of a non-Newtonian viscoelastic fluid over a stretching sheet in the presence of nonuniform radiation and heat source. Hari et al. [19] numerically analyzed the effect of chemical reaction on MHD mixed convective flow over a vertical plate embedded in a porous medium with thermal radiation. The velocity and concentration increase on increasing the values of the chemical reaction parameter in the case of generative case and they are decreasing in the case of destructive case. Makinde and Sibanda [20] investigated the effects of chemical reaction and internal heat generation on the boundary layer flow over a linearly stretching sheet. The local skin friction and mass transfer rate increase on increasing the Schmidt number. Bhattacharyya and Layek [21] analyzed steady, laminar stagnation-point flow in a porous shrinking sheet with radiation and suction. Wang [22] and Labropulu and Li [23] examined the effect of slip of a non-Newtonian fluid behavior at a stagnation-point flow over a plate. Harris et al. [24] and Bhattacharyya et al. [25] explored the steady mixed convection flow at a stagnation-point in a porous medium over a perpendicular surface with velocity slip condition. Merkin et al. [26] and Rohni et al. [27] considered temperature slip effect on an unsteady boundary layer flow in a porous medium. Aman et al. [28] and Seini and Makinde [29] studied the MHD flow of an incompressible fluid over a linearly shrinking/stretching sheet with slip effects. Singh and Chamkha [30] examined the heat transfer and fluid flow near the vertical linear shrinking sheet using second-order slip condition. They noticed that the skin friction falls on increasing the slip parameter. Roşca and Pop [31] explored steady forced flow and convection heat transfer over a vertical shrinking/stretching sheet using slip condition.

Inspired by the above applications and surveys explained, the purpose of this present study is to explore the effects of chemical reaction and velocity slip on mixed convection stagnation-point flow over a vertical plate embedded in a porous medium in the presence of external magnetic field and thermal radiation.

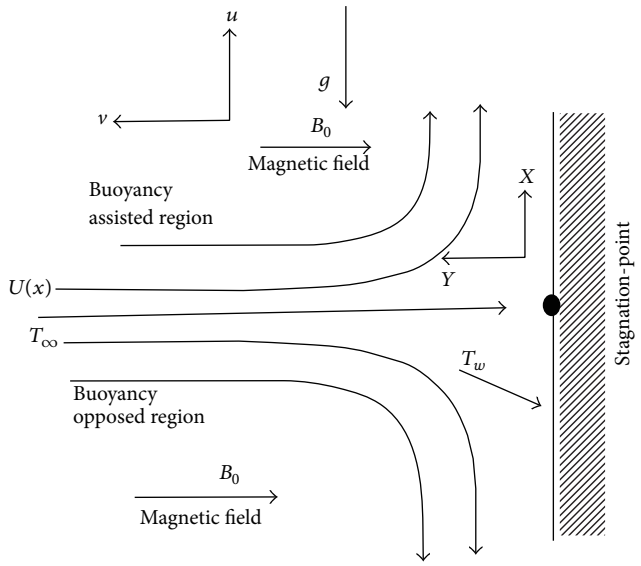

Figure 1: Schematic diagram of the problem.

2. Mathematical Model

Consider a steady, 2D laminar, mixed convection boundary layer flow of an incompressible viscous fluid near a stagnation-point along a vertical plate in the presence of magnetic field through a porous medium as exposed in Figure 1. It is presumed that the chemical reaction is considered as homogeneous and of first order. It is supposed that the porous medium is heat generating or absorbing internally at a fixed rate. Constant strength is enforced on unvarying magnetic field along the y-axis. The induced magnetic field is negligible due to small magnetic Reynolds number. As the fluid hits the wall at the stagnation-point, the flow is divided into two equal and opposite forces. In the potential flow region, the velocity distribution is assumed as $U_\infty = cx$, where c is a positive constant. The porous medium has isotropic, homogeneous, and thermodynamic equilibrium with local fluid. Therefore, the governing equations are given by

$$u_x + v_y = 0, \tag{1}$$

$$uu_x + vu_y = \upsilon u_{yy} + g\beta^* (C - C_\infty) + g\beta (T - T_\infty) - (u - U_\infty)\left(\frac{\sigma_e {B_0}^2}{\rho} + \frac{\upsilon}{\bar{K}}\right) + U_\infty \frac{dU_\infty}{dx}, \tag{2}$$

$$uT_x + vT_y = \alpha T_{yy} - \frac{1}{\rho C_p}\frac{\partial q_r}{\partial y} + \frac{Q(T - T_\infty)}{\rho C_p}, \tag{3}$$

$$uC_x + vC_y = DC_{yy} - \Gamma_0 (C - C_\infty). \tag{4}$$

Subject to the boundary conditions

$$\begin{aligned} u &= N_1 u_y, \\ v &= 0, \\ C &= C_w, \\ T &= T_w, \\ &\text{at } y = 0, \\ u &\longrightarrow U_\infty = cx, \\ C &\longrightarrow C_\infty, \\ T &\longrightarrow T_\infty, \\ &\text{as } y \longrightarrow \infty, \end{aligned} \tag{5}$$

the medium is taken to be gray, and emitting radiation and heat flux in the equation of energy due to thermal radiation are given by means of the Rosseland approximation:

$$q_r = -\frac{4\sigma^*}{3K'}\frac{\partial T^4}{\partial y}. \tag{6}$$

It is presumed that the transformation in temperature within the flow is too small, so that the temperature term T^4 might be stated as a linear combination of temperature (T) about free stream temperature (T_∞) using Taylor series and ignoring higher terms; we may express it as $T^4 \approx 4T_\infty^3 T - 3T_\infty^4$; we get

$$q_r = -\frac{16\sigma^* T_\infty^3}{3K'}T_y. \tag{7}$$

We declare the ensuing nondimensional variables to nondimensionalise the governing equations:

$$\begin{aligned} b &= N_1\left(\frac{c}{\nu}\right)^{1/2}, \\ \mathrm{Cr} &= \frac{\Gamma_0}{c}, \\ \mathrm{Gr}_C &= \frac{g\beta^*\left(C_\omega - C_\infty\right)x^3}{v^2}, \\ \mathrm{Gr}_T &= \frac{g\beta\left(T_\omega - T_\infty\right)x^3}{v^2}, \\ K &= \frac{v}{c\widetilde{K}}, \\ M &= \frac{\sigma_e B_0^2}{c\rho}, \\ \mathrm{Pr} &= \frac{v}{\alpha}, \\ \mathrm{Rd} &= \frac{4\sigma^* T_\infty^3}{kK'}, \\ \mathrm{Re}_x &= \frac{U_\infty x}{v}, \\ \mathrm{Ri}_C &= \frac{\mathrm{Gr}_C}{\mathrm{Re}_x^2}, \\ \mathrm{Ri}_T &= \frac{\mathrm{Gr}_T}{\mathrm{Re}_x^2}, \\ S &= \frac{Qv}{\rho C_p c}, \\ \mathrm{Sc} &= \frac{v}{D}, \\ \eta &= y\sqrt{\frac{c}{v}}, \\ \theta(\eta) &= \frac{T - T_\infty}{T_\omega - T_\infty}, \\ \phi(\eta) &= \frac{C - C_\infty}{C_\omega - C_\infty}, \\ \psi(x, y) &= \sqrt{vc}\,x f(\eta). \end{aligned} \tag{8}$$

Wherever the stream function (ψ) is defined in the normal notation as $u = \psi_y$ and $v = -\psi_x$, then the continuity equation (1) is satisfied. Replacing the expression in (7) together with (8) into (1)–(5), we attain the nonlinear ordinary differential equations:

$$f''' + ff'' - f'^2 + \mathrm{Ri}_T\theta + \mathrm{Ri}_C\phi - (K + M)\left(f' - 1\right) + 1 = 0, \tag{9}$$

$$\left(1 + \frac{4}{3}\mathrm{Rd}\right)\theta'' + \mathrm{Pr}f\theta' + S\theta = 0, \tag{10}$$

$$\phi'' + \mathrm{Sc}f\phi' - \mathrm{ScCr}\phi = 0. \tag{11}$$

By taking $(K + M) = M_p$ = porous-magnetic parameter and in (10) also considering $(1 + (4/3)\mathrm{Rd}) = RD$, (9) and (10) are modified as follows:

$$f''' + ff'' - f'^2 + \mathrm{Ri}_T\theta + \mathrm{Ri}_C\phi - M_p\left(f' - 1\right) + 1 = 0, \tag{12}$$

$$RD\theta'' + \mathrm{Pr}f\theta' + S\theta = 0. \tag{13}$$

The corresponding boundary conditions are

$$\begin{aligned} f &= 0, \\ f' &= bf''(0), \\ \theta &= 1, \\ \phi &= 1, \\ &\text{at } \eta = 0, \\ f' &= 1, \end{aligned}$$

$$\theta = 0,$$
$$\phi = 0,$$
$$\text{as } \eta \longrightarrow \infty. \tag{14}$$

The nondimensional numbers Cf_x, Nu, and Sh are defined as follows:

$$\mathrm{Cf}_x = \frac{2\tau_\omega}{\rho U_\infty^2},$$
$$\mathrm{Nu} = \frac{x q_\omega}{k\left(T_\omega - T_\infty\right)}, \tag{15}$$
$$\mathrm{Sh} = \frac{x q_m}{D\left(C_\omega - C_\infty\right)},$$
$$\tau_\omega = \mu \left.\frac{\partial u}{\partial y}\right|_{y=0},$$
$$q_\omega = -k \left.\frac{\partial T}{\partial y}\right|_{y=0} - \frac{4\sigma^*}{3K'} \left.\frac{\partial T^4}{\partial y}\right|_{y=0}, \tag{16}$$
$$q_m = -D \left.\frac{\partial C}{\partial y}\right|_{y=0}.$$

Substituting (7), (8), and (15) into (16), we receive the terms for the skin friction and local Nusselt and Sherwood numbers as follows:

$$\mathrm{Re}_x^{1/2}\mathrm{Cf}_x = f''(0),$$
$$\mathrm{Re}_x^{-1/2}\mathrm{Nu} = -R D \theta'(0), \tag{17}$$
$$\mathrm{Re}_x^{-1/2}\mathrm{Sh} = -\phi'(0).$$

3. Method of Solution

3.1. Analytical Solution by HAM. The analytical solutions of (11)–(13) along with the boundary conditions (14) are obtained by homotopy analysis method (HAM). The initial approximations for homotopy analysis solutions are chosen as

$$f_0(\eta) = \eta + \frac{e^{-\eta}}{1+b} - \frac{1}{1+b};$$
$$\theta_0(\eta) = e^{-\eta}; \tag{18}$$
$$\phi_0(\eta) = e^{-\eta}.$$

The auxiliary linear operators L_f, L_θ, and L_ϕ are

$$L_f = f''' - f';$$
$$L_\theta = \theta'' - \theta, \tag{19}$$
$$L_\phi = \phi'' - \phi,$$

satisfying the following properties:

$$L_f\left[C_1 + C_2 e^{\eta} + C_3 e^{-\eta}\right] = 0;$$
$$L_\theta\left[C_4 e^{\eta} + C_5 e^{-\eta}\right] = 0; \tag{20}$$
$$L_\phi\left[C_6 e^{\eta} + C_7 e^{-\eta}\right] = 0,$$

where C_i $(i = 1\text{–}7)$ denote the arbitrary constants. The zeroth-order deformation problems are

$$(1-p) L_f\left[\overline{f}(\eta, p) - f_0(\eta)\right] = p h_f N_f\left[\overline{f}(\eta, p), \overline{\theta}(\eta, p), \overline{\phi}(\eta, p)\right],$$
$$(1-p) L_\theta\left[\overline{\theta}(\eta, p) - \theta_0(\eta)\right] = p h_\theta N_\theta\left[\overline{f}(\eta, p), \overline{\theta}(\eta, p), \overline{\phi}(\eta, p)\right],$$
$$(1-p) L_\phi\left[\overline{\phi}(\eta, p) - \phi(\eta)\right] = p h_\phi N_\phi\left[\overline{f}(\eta, p), \overline{\theta}(\eta, p), \overline{\phi}(\eta, p)\right],$$
$$\overline{f}(0, p) = 0, \tag{21}$$
$$\overline{f}'(0, p) = \overline{bf}''(0, p),$$
$$\overline{f}'(\infty, p) = 1,$$
$$\overline{\theta}(0, p) = 1,$$
$$\overline{\theta}(\infty, p) = 0,$$
$$\overline{\phi}(0, p) = 1,$$
$$\overline{\phi}(\infty, p) = 0.$$

The mth-order deformation problem is of the form

$$L_f\left[f_m(\eta) - \chi_m f_{m-1}(\eta)\right] = h_f R_m^f(\eta) \tag{22}$$
$$L_\theta\left[\theta_m(\eta) - \chi_m \theta_{m-1}(\eta)\right] = h_\theta R_m^\theta(\eta) \tag{23}$$
$$L_\phi\left[\phi_m(\eta) - \chi_m \phi_{m-1}(\eta)\right] = h_\phi R_m^\phi(\eta) \tag{24}$$
$$f_m(0) = 0,$$
$$f_m'(0) = b f_m''(0),$$
$$\theta_m(0) = 0,$$
$$\phi_m(0) = 0, \tag{25}$$
$$f_m'(\infty) = 0,$$
$$\theta_m(\infty) = 0,$$
$$\phi_m(\infty) = 0,$$

Table 1: Comparison of analytical and numerical values of f'', $-\theta'$, and $-\phi'$ for different values of S when $\mathrm{Ri}_T = 1$, $\mathrm{Ri}_C = 0.5$, Pr = 1, Sc = 0.5, $M = 0$, $K = 0$, Cr = 0, and Rd = 0 with Makinde [14].

S	$f''(0)$			$-\theta'(0)$			$-\phi'(0)$		
	HAM	RK4	Makinde [14]	HAM	RK4	Makinde [14]	HAM	RK4	Makinde [14]
−1	1.9164	1.8501	1.8444	1.1215	1.3897	1.3908	0.4744	0.4618	0.4631
0	2.0158	1.9989	1.9995	0.6333	0.6401	0.6932	0.4814	0.4761	0.4789
1	2.0705	2.1299	2.1342	−0.1055	−0.0727	−0.0730	0.5062	0.4902	0.4917

Table 2: Analytical and numerical solutions for various values of $f''(0)$ when $K = 1$, $M = 1$, Pr = 7.2, and Sc = 1.0.

S	Rd	Cr	b	$f''(0)$		Error (%)
				HAM	RK4	
−1.5	1.0	0.5	0.4	1.741935	1.742816	0.05055
−1.0				1.745303	1.746196	0.05114
0.0				1.748974	1.749733	0.04338
1.0				1.752804	1.753440	0.03627
1.5				1.756711	1.757330	0.03522
0.5	0.0	0.5	0.4	1.696237	1.697773	0.09047
	0.3			1.718371	1.719537	0.06780
	0.5			1.731982	1.731025	0.05528
	0.8			1.744971	1.745330	0.02057
	1.5			1.770112	1.770255	0.08078
	2.0			1.782315	1.783635	0.07400
0.5	1.0	−2.0	0.4	2.061214	2.060439	0.03761
		−1.5		1.925079	1.924475	0.03139
		−0.5		1.805891	1.805358	0.02952
		0		1.774912	1.775401	0.02754
		0.5		1.752906	1.753440	0.03045
		1.5		1.723012	1.722443	0.03303
		2.0		1.711073	1.710801	0.01589
0.5	1.0	0.5	0.0	3.158507	3.157450	0.03347
			0.2	2.273258	2.272768	0.02156
			0.6	1.422014	1.421517	0.03496
			0.8	1.194172	1.193269	0.07567
			1.0	1.028569	1.027359	0.11777

Table 3: Analytical and numerical solutions for various values of $-\theta'(0)$ when $K = 1$, $M = 1$, Pr = 7.2, and Sc = 1.0.

S	Rd	Cr	b	$-\theta'(0)$		Error (%)
				HAM	RK4	
−1.5	1.0	0.5	0.4	1.503127	1.502298	0.05518
−1.0				1.439975	1.439975	0.00000
0.0				1.375810	1.375810	0.00000
1.0				1.309663	1.309663	0.00000
1.5				1.241382	1.241382	0.00000
0.5	0.0	0.5	0.4	1.912091	1.911775	0.01653
	0.3			1.646183	1.645690	0.02995
	0.5			1.523071	1.522510	0.03684
	0.8			1.383101	1.382877	0.01619
	1.5			1.169021	1.169727	0.06035
	2.0			1.068943	1.068377	0.05297
0.5	1.0	−2.0	0.4	1.445169	1.444713	0.03156
		−1.5		1.387088	1.386636	0.03259
		−0.5		1.334001	1.333199	0.06015
		0		1.319987	1.319596	0.02963
		0.5		1.309897	1.309663	0.01786
		1.5		1.296015	1.295783	0.01790
		2.0		1.291136	1.290635	0.03881
0.5	1.0	0.5	0.0	1.018166	1.017375	0.07775
			0.2	1.209972	1.209753	0.01810
			0.6	1.370195	1.369418	0.05673
			0.8	1.409185	1.408859	0.02313
			1.0	1.437043	1.436746	0.02067

where

$$
\begin{aligned}
R_m^f(\eta) &= f_{m-1}'''(\eta) \\
&\quad + \sum_{k=0}^{m-1} \left(f_{m-1-k}(\eta) f_k''(\eta) - f_{m-1-k}'(\eta) f_k'(\eta) \right) \\
&\quad + \mathrm{Ri}_T \theta + \mathrm{Ri}_C \phi - (Mp) f_{m-1}'(\eta) \\
&\quad + (Mp + 1)(1 - \chi_m), \\
R_m^\theta(\eta) &= \left(1 + \frac{4}{3}\mathrm{Rd}\right) \theta_{m-1}''(\eta) \\
&\quad + \mathrm{Pr} \sum_{k=0}^{m-1} f_{m-1-k}(\eta) \theta_k'(\eta) + S\theta_{m-1}(\eta), \\
R_m^\phi(\eta) &= \phi_{m-1}''(\eta) + \mathrm{Pr} \sum_{k=0}^{m-1} f_{m-1-k}(\eta) \phi_k'(\eta) - \mathrm{ScCr}\phi, \\
\chi_m &= \begin{cases} 0, & m \le 1 \\ 1, & m > 1. \end{cases}
\end{aligned}
\tag{26}
$$

The general solutions of (22)–(24) are

$$
\begin{aligned}
f_m(\eta) &= f^*{}_m(\eta) + C_1 + C_2\eta + C_3 e^{-\eta}, \\
\theta_m(\eta) &= \theta^*{}_m(\eta) + C_4 e^{\eta} + C_5 e^{-\eta}, \\
\phi_m(\eta) &= \phi^*{}_m(\eta) + C_6 e^{\eta} + C_7 e^{-\eta},
\end{aligned}
\tag{27}
$$

where $f^*{}_m(\eta)$, $\theta^*{}_m(\eta)$, and $\phi^*{}_m(\eta)$ are the special solutions. The symbolic calculations are obtained by MATLAB. Figure 2

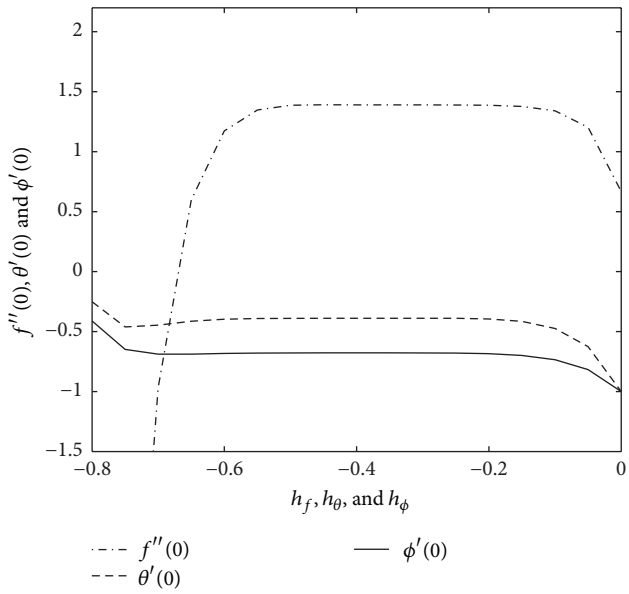

Figure 2: h curves of $f''(0)$, $\theta'(0)$, and $\phi'(0)$.

indicates that the respective admissible values of h_f, h_θ, and h_ϕ are $-0.5 \le h_f \le -0.2$ and $-0.6 \le h_\theta, h_\phi \le -0.2$. We choose the values of auxiliary parameter ($h = -0.35$) from this range; we will get the more accurate results.

3.2. Numerical Method. The coupled equations (11)–(13) along with the boundary conditions (14) are transformed into the linear differential equations by defining dependent variables of first order. The set of coupled linear differential equations of first-order system are integrated using Runge-Kutta fourth-order method from $\eta = 0$ to $\eta = \eta_{\max}$ by taking consecutive steps $\Delta\eta$. The assumed initial values of $f''(0)$, $\theta'(0)$, and $\phi'(0)$ are compared with the measured values of $f''(0)$, $\theta'(0)$, and $\phi'(0)$ at $\eta = \eta_{\max}$. If the dissimilarity is present, assume another set of primary values for $f''(0)$, $\theta'(0)$, and $\phi'(0)$ and the procedure is repeated. This process is repeated up to the arrangement between considered value and the agreed condition at $\eta = \eta_{\max}$ within the degree of exactness. The analytical and numerical results are compared with the results available in the literature and they are shown in Table 1. This provides confidence in our analytical and numerical results to be reported subsequently.

4. Results and Discussion

Analytical solution by using HAM and numerical solution by using shooting method were obtained for different values of radiation, chemical reaction, and velocity slip parameters. The values of the parameters $\mathrm{Ri}_T = 2.0$, $\mathrm{Ri}_C = 2.0$, $M_p = 2.0$, Pr = 7.2, and Sc = 1 are fixed throughout the study. Tables 2–4 depict the values of $f''(0)$, $-\theta'(0)$, and $-\phi'(0)$ from the analytical and numerical methods. Table 2 depicts that skin friction increases on increasing the internal heat generation (S) and radiation (Rd) parameters. It is inferred that the skin friction decreases on increasing the chemical reaction (Cr) and slip (b) parameters. Tables 3 and 4 show that the heat transfer rate decreases and the mass transfer rate increases on increasing S, Rd, and Cr parameters. It is noticed that the mass and heat transfer rates increase on increasing the slip parameter (b).

Table 4: Analytical and numerical solutions for various values of $-\phi'(0)$ when $K = 1$, $M = 1$, Pr = 7.2, and Sc = 1.0.

S	Rd	Cr	b	$-\phi'(0)$		Error (%)
				HAM	RK4	
−1.5	1.0	0.5	0.4	1.044089	1.043630	0.04398
−1.0				1.045321	1.044155	0.11166
0.0				1.045172	1.044706	0.04460
1.0				1.046004	1.045285	0.06878
1.5				1.046148	1.045894	0.02428
0.5	0.0	0.5	0.4	1.036874	1.036006	0.08378
	0.3			1.039876	1.039445	0.04146
	0.5			1.042083	1.041357	0.06971
	0.8			1.044115	1.043834	0.02692
	1.5			1.049270	1.048402	0.08279
	2.0			1.051298	1.050986	0.02968
0.5	1.0	−2.0	0.4	−1.559173	−1.564133	0.31710
		−1.5		−0.489101	−0.490619	0.30940
		−0.5		0.513916	0.514218	0.05872
		0		0.808952	0.808147	0.09961
		0.5		1.046013	1.045285	0.06964
		1.5		1.425416	1.424446	0.06809
		2.0		1.585091	1.584309	0.04935
0.5	1	0.5	0.0	0.949062	0.948406	0.06916
			0.2	1.012067	1.011676	0.03864
			0.6	1.066135	1.065652	0.04532
			0.8	1.079006	1.079208	0.01871
			1.0	1.089222	1.088848	0.03434

Figure 3(a) illustrates profiles of velocity along the boundary layer for Rd = 0.3, S = 1.5, and Cr = 0.3 and different values of slip parameter. The velocity increases as the slip parameter is increased. The boundary layer thickness increases when the slip parameter is increased. Figures 3(b) and 3(c) show the influence of slip parameter on temperature as well as concentration, respectively. These two profiles decrease on increasing the slip parameter. This is the reason why the viscosity decreases in the medium or the free stream velocity increases, and it results in the thermal and solutal boundary layer thickness decrease. The velocity and temperature profiles for various values of radiation parameter (Rd) are illustrated in Figures 4(a) and 4(b). As the radiation increases, the velocity as well as temperature increases significantly. The thickness of the thermal boundary layer increases on increasing the radiation parameter because the intensity of the electromagnetic radiation in the medium decreases and the Stefan-Boltzmann constant of the medium increases. Figures 5(a) and 5(b) depict the chemical reaction effect on both the velocity and concentration profiles along the surface for constant values of radiation (Rd = 1.0), internal heat generation (S = 1.0), and slip parameter

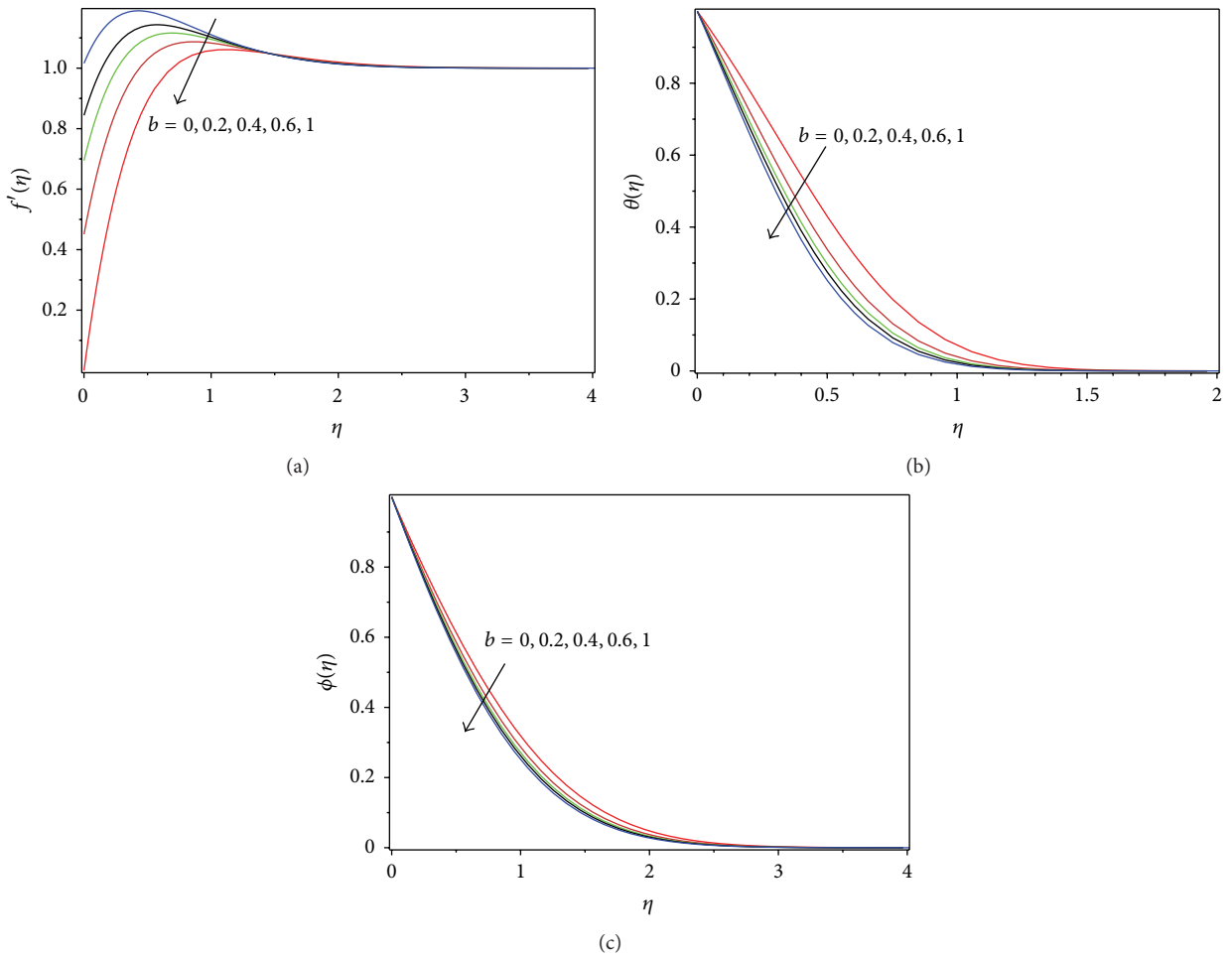

FIGURE 3: Velocity (a), temperature (b), and concentration (c) profiles for different values of slip parameter with $S = 1.5$, Rd $= 0.3$, and Cr $= 0.3$.

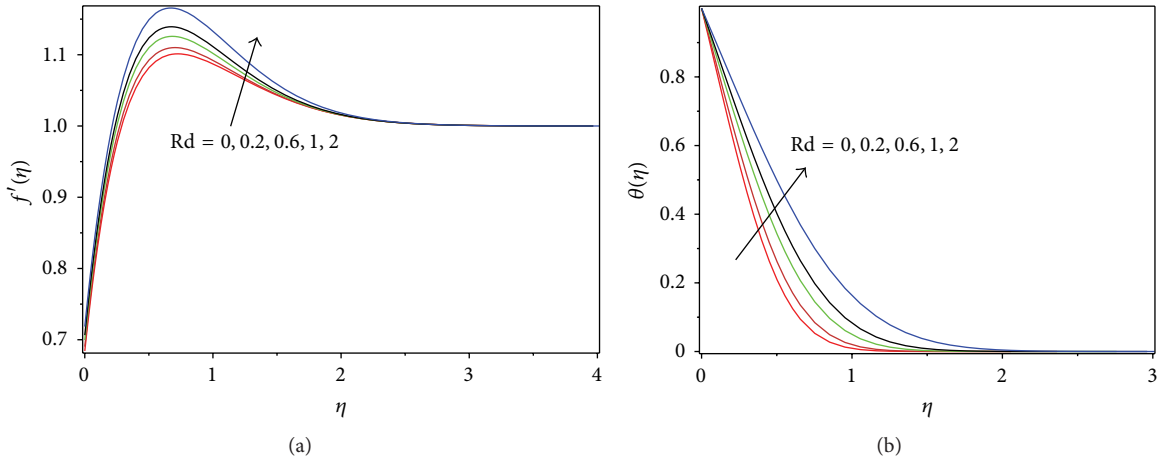

FIGURE 4: Velocity (a) and temperature (b) profiles for different values of radiation parameter with $S = 1.0$, Cr $= 0.3$, and $b = 0.4$.

($b = 0.4$). The velocity and concentration increase on increasing the chemical reaction parameter. The concentration profile overshoots in the generative chemical reaction case, that is, the negative values of the chemical reaction parameter.

It can be observed from Figures 6(a)–6(c) that the local skin friction decreases on increasing the chemical reaction parameter and slip parameter. As the radiation increases, local skin friction increases due to temperature gradient causes in the fluid. In Figures 7(a)–7(c), it is interesting to

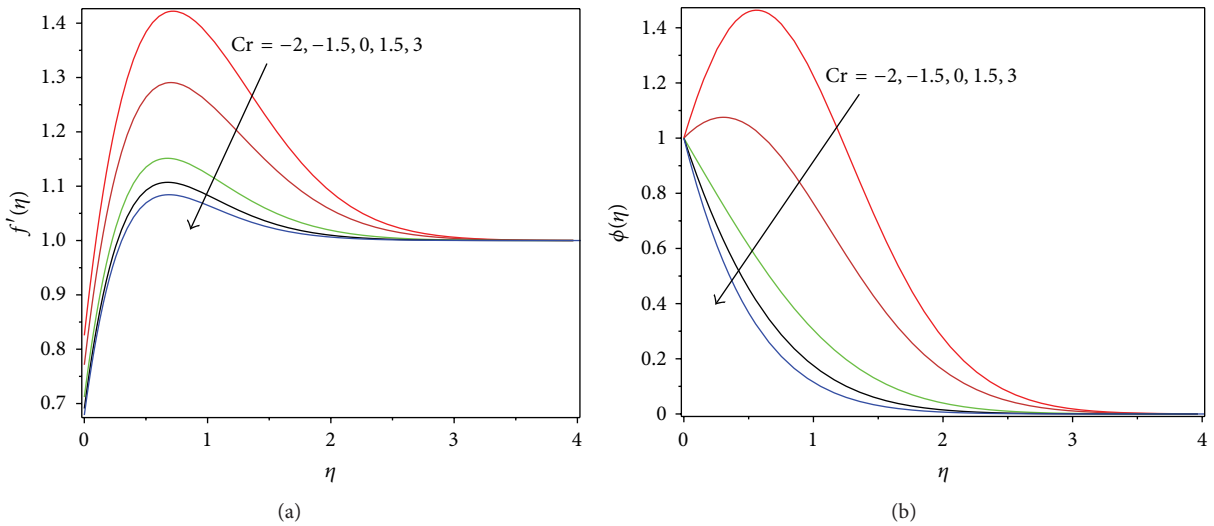

Figure 5: Velocity (a) and concentration (b) profiles for different values of chemical reaction parameter with $S = 1.0$, Rd = 1.0, and $b = 0.4$.

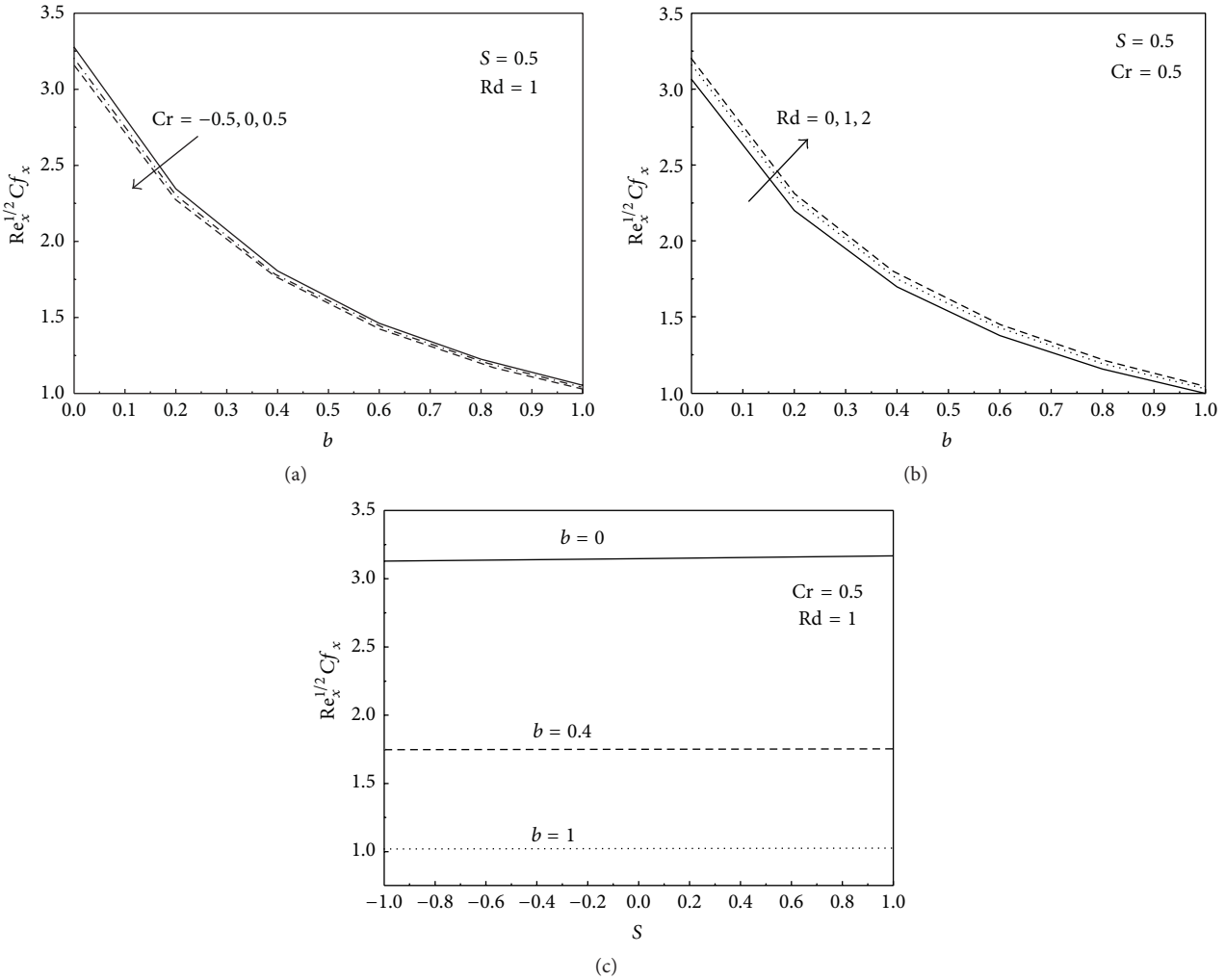

Figure 6: Local skin friction for different (a) chemical reaction parameter with $S = 0.5$ and Rd = 1.0, (b) radiation parameter with $S = 0.5$ and Cr = 0.5, and (c) slip parameter with Cr = 0.5 and Rd = 1.0.

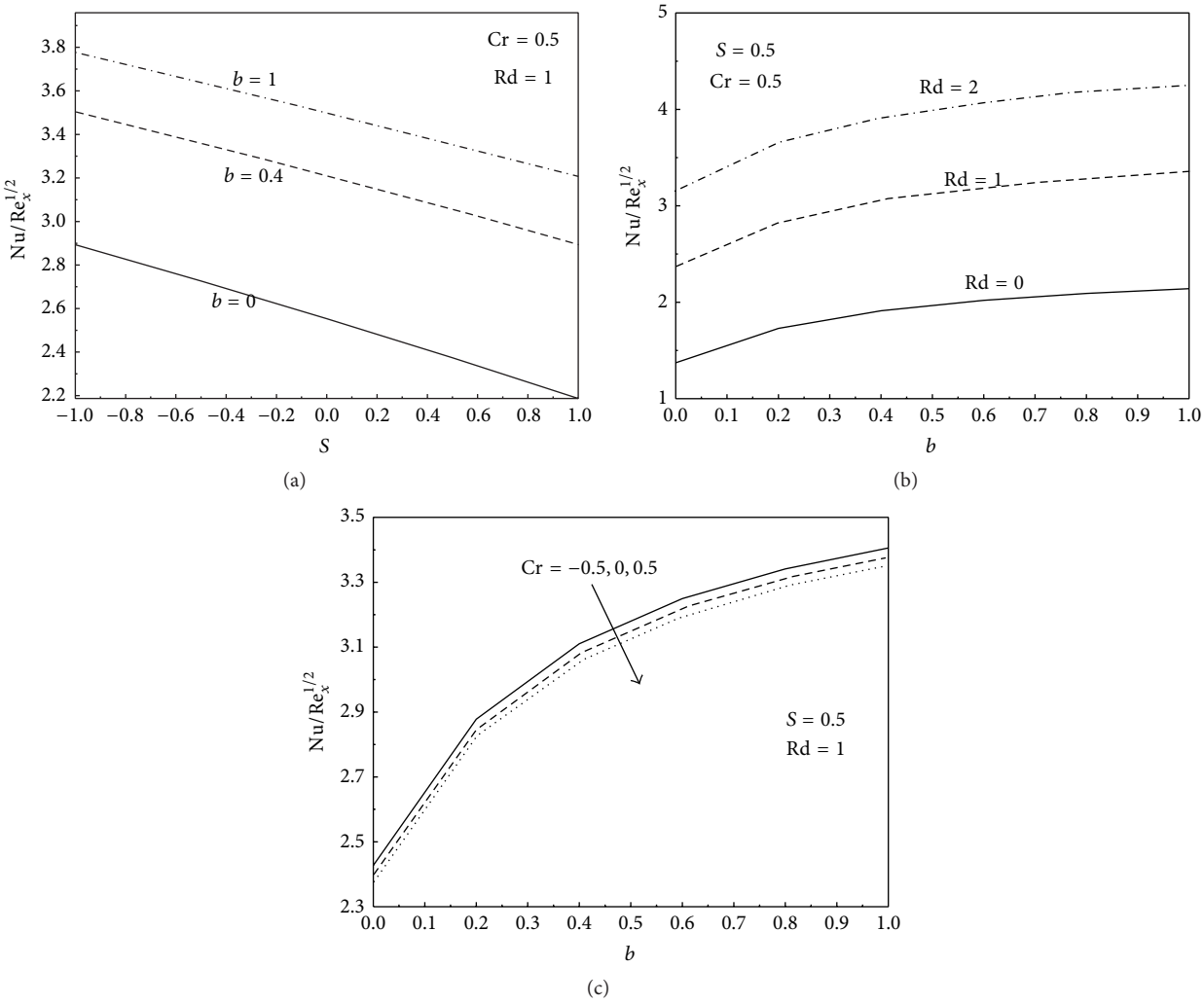

FIGURE 7: Local Nusselt numbers for different (a) slip parameter with Cr = 0.5 and Rd = 1.0, (b) radiation parameter with $S = 0.5$ and Cr = 0.5, and (c) chemical reaction parameter with $S = 0.5$ and Rd = 1.0.

note that Nusselt number increases on increasing the slip and radiation parameters. However, as the chemical reaction parameter increases, the local Nusselt number decreases. It is interesting to note that the local heat transfer rate decreases on increasing the internal heat generation parameter. Figures 8(a)–8(c) show that the local Sherwood number increases on increasing the chemical reaction, radiation, and slip parameters. Further scrutinising these figures, it is found that the local mass transfer rate increases with slip parameter. However, the effect of internal heat generation on local mass transfer rate is negligible.

5. Conclusions

The effects of chemical reaction and slip parameters on magnetoconvection stagnation-point flow in a porous medium over a vertical plate with thermal radiation are investigated. The governing equations are solved analytically using HAM and numerically by shooting technique along with Runge-Kutta fourth-order integration. The results show a good agreement between the analytical and numerical results of the considered problem. The velocity increases on increasing the slip and radiation parameters and it increases on decreasing the chemical reaction parameter. The temperature decreases on increasing the slip parameter and it increases on increasing the radiation parameter. The concentration increases on decreasing the chemical reaction parameter and it decreases on increasing the slip parameter. The skin friction decreases on increasing the slip and chemical reaction parameters. The local mass and heat transfer rates increase on increasing the slip parameter.

Nomenclature

b : Slip parameter
B_0: Strength of the magnetic field
C: Species concentration
Cr: Chemical reaction parameter
D: Diffusion coefficient
f: Dimensionless stream function

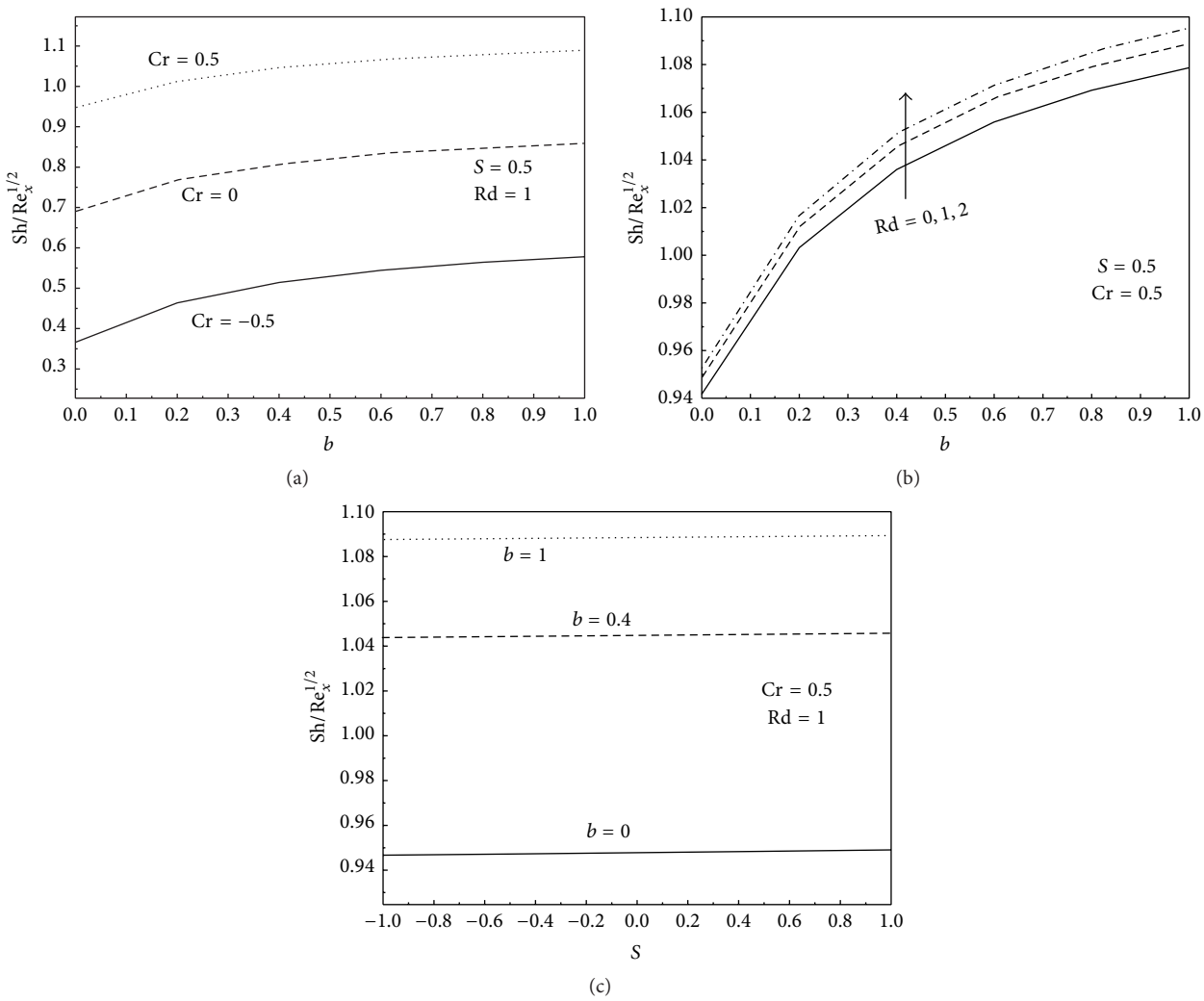

Figure 8: Local Sherwood numbers for different (a) chemical reaction parameter with $S = 0.5$ and $\mathrm{Rd} = 1.0$, (b) radiation parameter with $S = 0.5$ and $\mathrm{Cr} = 0.5$, and (c) slip parameter with $\mathrm{Cr} = 0.5$ and $\mathrm{Rd} = 1.0$.

g: Gravitational acceleration
Gr_C: Solutal Grashof number
Gr_T: Thermal Grashof number
k: Thermal conductivity
K: Permeability parameter
$\widetilde{K}$: Porous medium permeability
K': Mean absorption coefficient
M: Magnetic field parameter
N_1: Navier slip coefficient
Nu: Nusselt number
Pr: Prandtl number
Q: Heat generation/absorption
Rd: Thermal radiation parameter
Re_x: Reynolds number
Ri_T: Thermal Richardson number
Ri_C: Solutal Richardson number
S: Heat generation parameter
Sc: Schmidt number
Sh: Sherwood number
T: Temperature
u, v: Velocity components
x, y: Cartesian coordinates.

Greek Symbols

β: Coefficient of thermal expansion
β^*: Coefficient of solutal expansion
Γ_0: Chemical reaction rate
η: Similarity variable
θ: Dimensionless temperature
μ: Dynamic viscosity
υ: Kinematic viscosity
ρ: Density
σ^*: Stefan-Boltzmann constant
σ_e: Electrical conductivity

ϕ: Dimensionless concentration
ψ: Stream function.

Subscripts

w: At wall
∞: At free stream.

Competing Interests

The authors declare that they have no competing interests.

References

[1] K. Hiemenz, "Die Grenzschicht an einem in den gleichformingen Flussigkeitsstrom einge-tauchten geraden Kreiszylinder," *Dingler's Polytechnisches Journal*, vol. 3326, pp. 321–324, 1911.

[2] L. J. Crane, "Flow past a stretching plate," *Zeitschrift für angewandte Mathematik und Physik ZAMP*, vol. 21, no. 4, pp. 645–647, 1970.

[3] F. Mohammadi, "A computational approach for solution of boundary layer equations for the free convection along a vertical plate," *Journal of Computational Methods in Sciences and Engineering*, vol. 15, no. 3, pp. 317–326, 2015.

[4] J. Cheng, S. Liao, and I. Pop, "Analytic series solution for unsteady mixed convection boundary layer flow near the stagnation point on a vertical surface in a porous medium," *Transport in Porous Media*, vol. 61, no. 3, pp. 365–379, 2005.

[5] G. C. Layek, S. Mukhopadhyay, and S. A. Samad, "Heat and mass transfer analysis for boundary layer stagnation-point flow towards a heated porous stretching sheet with heat absorption/generation and suction/blowing," *International Communications in Heat and Mass Transfer*, vol. 34, no. 3, pp. 347–356, 2007.

[6] J. Lee, P. Kandaswamy, M. Bhuvaneswari, and S. Sivasankaran, "Lie group analysis of radiation natural convection heat transfer past an inclined porous surface," *Journal of Mechanical Science and Technology*, vol. 22, no. 9, pp. 1779–1784, 2008.

[7] M. Ferdows, K. Kaino, and S. Sivasankaran, "Free convection flow in an inclined porous surface," *Journal of Porous Media*, vol. 12, no. 10, pp. 997–1003, 2009.

[8] H. Rosali, A. Ishak, and I. Pop, "Mixed convection stagnation-point flow over a vertical plate with prescribed heat flux embedded in a porous medium: brinkman-extended Darcy formulation," *Transport in Porous Media*, vol. 90, no. 3, pp. 709–719, 2011.

[9] S.-S. Hou, "Analysis of a stagnation-point premixed flame influenced by inert spray, heat loss, and non-unity Lewis number," *Applied Mathematical Modelling*, vol. 37, no. 3, pp. 1333–1346, 2013.

[10] M. Bhuvaneswari, S. Sivasankaran, and Y. J. Kim, "Lie group analysis of radiation natural convection flowover an inclined surface in a porous medium with internal heat generation," *Journal of Porous Media*, vol. 15, no. 12, pp. 1155–1164, 2012.

[11] H. S. Takhar, A. J. Chamkha, and G. Nath, "Unsteady mixed convection on the stagnation-point flow adjacent to a vertical plate with a magnetic field," *Heat and Mass Transfer*, vol. 41, no. 5, pp. 387–398, 2005.

[12] O. Aydin and A. Kaya, "MHD mixed convection of a viscous dissipating fluid about a permeable vertical flat plate," *Applied Mathematical Modelling*, vol. 33, no. 11, pp. 4086–4096, 2009.

[13] T. Hayat, Z. Abbas, I. Pop, and S. Asghar, "Effects of radiation and magnetic field on the mixed convection stagnation-point flow over a vertical stretching sheet in a porous medium," *International Journal of Heat and Mass Transfer*, vol. 53, no. 1–3, pp. 466–474, 2010.

[14] O. D. Makinde, "Heat and mass transfer by MHD mixed convection stagnation point flow toward a vertical plate embedded in a highly porous medium with radiation and internal heat generation," *Meccanica*, vol. 47, no. 5, pp. 1173–1184, 2012.

[15] M. Bhuvaneswari, S. Sivasankaran, and M. Ferdows, "Lie group analysis of natural convection heat and mass transfer in an inclined surface with chemical reaction," *Nonlinear Analysis: Hybrid Systems*, vol. 3, no. 4, pp. 536–542, 2009.

[16] K. Bhattacharyya, "Dual solutions in boundary layer stagnation-point flow and mass transfer with chemical reaction past a stretching/shrinking sheet," *International Communications in Heat and Mass Transfer*, vol. 38, no. 7, pp. 917–922, 2011.

[17] A. A. Afify and N. S. Elgazery, "Lie group analysis for the effects of chemical reaction on MHD stagnation-point flow of heat and mass transfer towards a heated porous stretching sheet with suction or injection," *Nonlinear Analysis: Modelling and Control*, vol. 17, no. 1, pp. 1–15, 2012.

[18] M. S. Abel and N. Mahesha, "Heat transfer in MHD viscoelastic fluid flow over a stretching sheet with variable thermal conductivity, non-uniform heat source and radiation," *Applied Mathematical Modelling*, vol. 32, no. 10, pp. 1965–1983, 2008.

[19] N. Hari, S. Sivasankaran, M. Bhuvaneswari, and Z. Siri, "Effects of chemical reaction on MHD mixed convection stagnation point flow toward a vertical plate in a porous medium with radiation and heat generation," *Journal of Physics: Conference Series*, vol. 662, no. 1, Article ID 012014, pp. 1–9, 2015.

[20] O. D. Makinde and P. Sibanda, "Effects of chemical reaction on boundary layer flow past a vertical stretching surface in the presence of internal heat generation," *International Journal of Numerical Methods for Heat and Fluid Flow*, vol. 21, no. 6, pp. 779–792, 2011.

[21] K. Bhattacharyya and G. C. Layek, "Effects of suction/blowing on steady boundary layer stagnation-point flow and heat transfer towards a shrinking sheet with thermal radiation," *International Journal of Heat and Mass Transfer*, vol. 54, no. 1–3, pp. 302–307, 2011.

[22] C. Y. Wang, "Stagnation flows with slip: exact solutions of the Navier-Stokes equations," *Zeitschrift für angewandte Mathematik und Physik ZAMP*, vol. 54, no. 1, pp. 184–189, 2003.

[23] F. Labropulu and D. Li, "Stagnation-point flow of a second-grade fluid with slip," *International Journal of Non-Linear Mechanics*, vol. 43, no. 9, pp. 941–947, 2008.

[24] S. D. Harris, D. B. Ingham, and I. Pop, "Mixed convection boundary-layer flow near the stagnation point on a vertical surface in a porous medium: brinkman model with slip," *Transport in Porous Media*, vol. 77, no. 2, pp. 267–285, 2009.

[25] K. Bhattacharyya, S. Mukhopadhyay, and G. C. Layek, "Slip effects on boundary layer stagnation-point flow and heat transfer towards a shrinking sheet," *International Journal of Heat and Mass Transfer*, vol. 54, no. 1–3, pp. 308–313, 2011.

[26] J. H. Merkin, A. M. Rohni, S. Ahmad, and I. Pop, "On the temperature slip boundary condition in a mixed convection boundary-layer flow in a porous medium," *Transport in Porous Media*, vol. 94, no. 1, pp. 133–147, 2012.

[27] A. M. Rohni, S. Ahmad, I. Pop, and J. H. Merkin, "Unsteady mixed convection boundary-layer flow with suction and temperature slip effects near the stagnation point on a vertical permeable surface embedded in a porous medium," *Transport in Porous Media*, vol. 92, no. 1, pp. 1–14, 2012.

[28] F. Aman, A. Ishak, and I. Pop, "Magnetohydrodynamic stagnation-point flow towards a stretching/shrinking sheet with slip effects," *International Communications in Heat and Mass Transfer*, vol. 47, pp. 68–72, 2013.

[29] I. Y. Seini and D. O. Makinde, "Boundary layer flow near stagnation-points on a vertical surface with slip in the presence of transverse magnetic field," *International Journal of Numerical Methods for Heat & Fluid Flow*, vol. 24, no. 3, pp. 643–653, 2014.

[30] G. Singh and A. J. Chamkha, "Dual solutions for second-order slip flow and heat transfer on a vertical permeable shrinking sheet," *Ain Shams Engineering Journal*, vol. 4, no. 4, pp. 911–917, 2013.

[31] A. V. Roşca and I. Pop, "Flow and heat transfer over a vertical permeable stretching/shrinking sheet with a second order slip," *International Journal of Heat and Mass Transfer*, vol. 60, no. 1, pp. 355–364, 2013.